Article

J. Mex. Chem. Soc. **2014**, *58(1),* 46-51

ISSN 1870-249X

A Theoretical Study of Lithium-intercalated Pristine and Doped Carbon Nanocones

Ali Ahmadi Peyghan[1] and Maziar Noei[2*]

[1] Young Researchers and Elite club, Central Tehran Branch, Islamic Azad University, Tehran, Iran
[2] Department of Chemistry, Mahshahr Branch, Islamic Azad University, Mahshahr, Iran. noeimaziar@gmail.com

Received February 7th, 2013; Accepted September 24th, 2013

Abstract. The energetic, geometric, and electronic structure of Li-adsorbed pristine, B- and N-doped carbon nanocones (B- and N-CNCs) were investigated by means of density functional theory. It was found that Li atom is strongly adsorbed above the center of pentagonal ring of the pristine CNC with the adsorption energy of −1.08 eV (at B3LYP/6-31G(d)) along with the charge transfer from Li to the CNC. After this process, the semiconductive CNC is transformed to an n-type one, so that its HOMO-LUMO energy gap (E_g) is reduced from 2.51 to 0.71 eV (at B3LYP/6-31G(d)). Doping semiconductive CNC with B or N atom also creates a p- or n-type semiconductive material, resulting in an increased conductance. B-doping improves the Li adsorption on the CNC, while N-doping hinders this process. It seems that Li atom acts as an electron-donor agent with n-type effect, and therefore, its adsorption on the B-CNC somewhat compensates the p-type effect of B-doping. On the contrary, the adsorption process on the N-CNC moderately promotes the n-type effect of N-doping, leading to more reduction in the E_g value.
Key words: Nanostructures, Adsorption; Density functional theory; Lithium battery

Resumen. La energética, así como las estructuras geométricas y electrónicas de Li adsorbido en nanoconos de carbono puros y dopados con B y N (B- and N-CNCs) se investigan por medio de la teoría de funcionales de la densidad. Se encontró que el átomo de Li se adsorbe fuertemente sobre el centro de un anillo pentagonal de un CNC puro con una energía de adsorción de −1.08 eV (utilizando B3LYP/6-31G(d)), junto con una transferencia de carga del Li al CNC. Después de este proceso, el CNC semiconductor se transforma en uno de tipo-n, de manera que la brecha de energía HOMO-LUMO (E_g) se redujo de 2.51 a 0.71 eV (utilizando B3LYP/6-31G(d)). Al dopar el CNC semiconductor con B o N también crea un material semicoductor tipo-p y -n, incrementando su conductancia. El dopaje con B mejora la adsorción de Li en el CNC, mientras que el dopaje con N dificulta este proceso. Parece que el átomo de Li actúa como un agente electrodonador con un efecto tipo-n, y por tanto, su adsorción sobre el B-CNC de alguna manera compensa el efecto tipo-p del dopaje con B. Por el contrario, el proceso de adsorción sobre el N-CNC promueve moderadamente el efecto tipo-n del dopaje con N, lo que lleva a una mayor reducción en el valor de E_g.
Palabras clave: Nanoestructuras, adsorción, teoría de funcionales de la densidad, batería de litio.

Introduction

The increasing demand for lithium ion batteries with high energy storage density, used in portable electronic devices, has spawned many explorations of new lithium intercalation materials with superior performance both as cathodes and anodes [1-4]. Currently, carbon based materials are the choice for lithium storage in Li-ion batteries [5, 6]. In Li-ion batteries, graphitic carbon anodes are used instead of metallic Li electrodes because of safety and cycle efficiency [7]. However, the use of graphite as a host material leads to a specific capacity reduction from 3860 mA h g^{-1} for metallic Li to 372 mA h g^{-1} for graphitic anodes [8]. Now, with the recent discovery of new crystalline forms of carbon, specifically carbon nanotubes (CNTs) with dimensions of 1-100 nm, it appears that there may be a new paradigm in carbon-based battery electrode materials. Recent experiments found much higher Li content ($Li_{1.6}C_6$) in CNTs than graphite (LiC_6) [9]. The Li content can be further improved up to $Li_{2.7}C_6$ via chemical etching or ball-milling of the nanotubes [10]. Zhao *et al.* have simulated Li intercalation in SWCNT bundles and have demonstrated the possibility of high saturation density of about Li_3C_6 [11]. In order to get higher Li capacity, B- or N-substitution in CNTs has been widely studied both experimentally and theoretically [12]. Different allotropes of carbon-based materials for Li battery have also been studied by many groups [13-15].

Following Iijima's discovery of CNT [16], researches on nanostructured compounds have been devoted to developing their large-scale synthesis and finding their novel applications in many areas of physics and chemistry [17-21]. Nanocones were observed for the first time in 1992 as caps at the ends of nanotubes [22] just after the discovery of CNTs, and they were observed as free standing structures two years later. Pincak and Osipov [23] have previously reported the results for the electronic structure of carbon nanocones. Charlier and Rignanese [24] studied the local density of states for the carbon nanocones using molecular dynamics. More recently, nanocones have started to be the focus of increasing scientific and technological interests because of their special electronic and mechanical features. These structures are believed to have numerous potential applications in the fields of nanoelectronics and nanomaterials science as well as molecular traps [25-28]. Recently, theoretical calculations on the pristine nanocone have shown that these nanostructures are very promising for hydrogen-storage applications [26]. However, to our knowledge, no experiment and theoretical investigation have been reported on Li storage which is important in the applications of re-chargeable batteries. Here, we present the results for the energetic,

geometric, and electronic structure of Li-intercalated pristine and boron- or nitrogen-doped carbon nanocones (CNC) using density functional theory (DFT) calculations. Our study can help the researchers working on the development of lithium ion batteries. Similar to the Li-intercalated CNTs [29], the CNC is expected to be a candidate for anode material in Li-ion battery applications.

Computational Methods

Full geometry optimizations on the pristine, B- and N-doped CNCs (B- and N-CNCs) in the presence and absence of a Li atom were performed using hybrid generalized gradient approximation with the B3LYP and the 6-31G (d) basis set. The B3LYP has been demonstrated to be a reliable and commonly used functional in the study of different nanostructures [30-33]. This functional has been previously calibrated for the interaction of Li atoms with five center carbon-based rings, i.e., polythiophene [34].Vibrational frequency calculations have been performed at the same level of theory to gain a qualitative idea of whether the final structures correspond to the minima on the potential energy surface. The smallest frequency modes were shown in Table 1. The adsorption energy (E_{ad}) of a Li atom is defined as follows:

$$E_{ad} = E_{(Li\text{-}CNC)} - E_{(Li)} - E_{(CNC)}$$

where $E_{(Li\text{-}CNC)}$ is the total energy of the Li-CNC complex, and $E_{(CNC)}$ or $E_{(Li)}$ is referred to the energy of an isolated CNC or Li atom. By the definition, a negative value of E_{ad} corresponds to an exothermic adsorption. The doping energy (E_{dop}) is also calculated as follows:

$$E_{dop} = E_{(doped\text{-}CNC)} + E_{(doping\ atom)} - E_{(C)} - E_{(CNC)}$$

where $E_{(doped\text{-}CNC)}$ is the total energy of the boron- or nitrogen-doped CNC, and $E_{(doping\ atom)}$ and $E_{(C)}$ are referred to the energy of a single doping atom (B or N) and C atom, respectively. All of the calculations were carried out using a locally modified version of the GAMESS electronic structure program [35].

Results and Discussion

At first, we have optimized the structure of pure CNC. Krishnan *et al.* have previously observed that the conical shape stems from 1 to 5 carbon pentagons incorporated into the graphene structure near the cone apex, giving rise to five discrete apex angles of 112.9°, 83.6°, 60.0°, 38.9°, and 19.2° [36]. Here, we have focused on the CNC with the cone angle of 112.9° (Fig. 1), which is the largest experimentally [36] and theoretically [37] observed angle. The proposed pristine CNC consists of 80 carbon atoms, and the dangling bonds of CNC are saturated with hydrogen atoms. The bottom carbon layer is fixed during the whole computation as well as hydrogen atoms. Several types of C-C bonds are observed through CNC with different lengths of 1.43 Å (C5-C6) and 1.36-1.45 Å (C6-C6). The carbons of pentagonal and hexagonal rings are denoted as C5 and C6, respectively.

A Li atom has been considered to be adsorbed on the outside surface of the CNC. We probed a number of different adsorption sites on the cone surface, for instance, the top (above the C5 atom) and bridge (above the C5-C5 bond) site in order to find the lowest-energy configuration for the adsorbate/adsorbent system. It is worth saying that we just focused on the apex of CNC for Li storage to predict the overall characteristics of pristine and doped cone. After careful structural optimization, we have found that the most favorable adsorption site is on the top of the pentagonal ring center with E_{ad} of −1.08 eV, and interestingly, in other configurations the target metal re-oriented to this stable site. In this configuration, the lowest length of Li-C is about 2.20 Å (Fig. 2) and a charge transfer of 0.38 *e* occurred from the atom to the CNC. It was also found that the adsorption induces little local structural deformation on CNC. The C5-C5 and C5-C6 bond lengths in the cone apex slightly changed from 1.43 and 1.39 Å to 1.43 and 1.41 Å, respectively. Further indication of deformation degree after the adsorption process is given by the bond reorganization energy (E_{br}), calculated as the energy difference between the geometry of the cone after the adsorption and the full relaxed one. The calculated E_{br} for CNC is about −1.21 eV. In Table 1, we have summarized the results for E_{ad}, NBO charge analysis, and HOMO/LUMO energy gap (E_g). It should be noted that the E_g also stands

Table 1. Adsorption energy of Li on pristine and B/N-doped CNC (E_{ad}), bond reorganization energy (E_{br}, calculated as the energy difference between the geometry of Li after adsorption on nanocone and the full relaxed molecule), NBO charge on the adsorbed Li (Q_T), the HOMO (or SOMO), LUMO and gap in between energies (E_g) for different Li/cone complexes at B3LYP/6-31G (d). Energies are in eV.

system	E_{ad}	E_{br}	Q_T (e)	υ_{min} (cm^{-1})	*E_{HOMO}	E_{LUMO}	E_g	**ΔE_g(%)
CNC	—	—	—	150.2	−5.00	−2.49	2.51	—
Li adsorbed CNC	−1.08	−1.21	0.42	98.5	−3.22	−2.48	0.74	70.5
B-CNC	—	—	—	145.3	−4.54	−3.51	1.03	—
Li adsorbed B-CNC	−2.49	−2.63	0.31	91.4	−4.50	−2.39	2.11	102.8
N-CNC	—	—	—	151.7	−3.53	−2.62	0.91	—
Li adsorbed N-CNC	−0.55	−0.67	0.33	96.2	−3.29	−2.47	0.82	9.9

*It also stands for the energy of SOMO.
**Change of E_g of cone after the adsorption of Li atom.

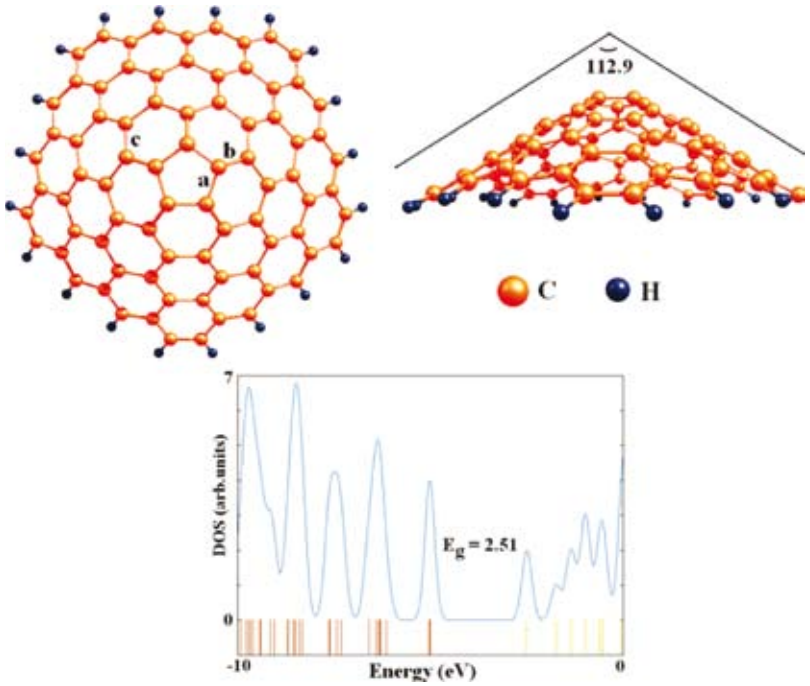

Fig. 1. Optimized structure of CNC and its DOS (arb.units). Bond lengths of a, b and c bonds are 1.43, 1.39 and 1.42 Å.

for SOMO (singly occupied molecular orbital) /LUMO energy gaps for the open shell systems.

In order to consider the influence of Li adsorption on the electronic properties of the cone, we have drawn the DOS plots for both the bare and metal adsorbed CNC as shown in Figs. 1 and 2. From the DOS plot of the bare CNC (Fig. 1), it can be concluded that it is a semiconductive material with E_g of 2.51 eV. As shown by panel b in Fig. 2, the DOS of the Li adsorbed configuration has a distinct change near the conduction level compared with that of the pristine CNC. After the Li adsorption, an impurity state is appeared within the E_g of CNC at the energy level of −3.22 eV, transforming the CNC from intrinsic to an *n*-type extrinsic semiconductor, so that the E_g of CNC is decreased from 2.51 to 0.74 eV (by about 70.5% change). This occurrence is expected to bring about obvious change in the corresponding electrical conductivity because it is well known that the E_g (or band gap in the bulk materials) is a major factor determining the electrical conductivity of the material and a classic relation between them is as follows [38]:

$$\sigma \propto \exp\left(\frac{-E_g}{2kT}\right) \tag{2}$$

where σ is the electrical conductance and *k* is the Boltzmann's constant. According to the equation, smaller E_g values lead to higher conductance at a given temperature. Therefore, the observed substantial E_g reduction of CNC after the adsorption process leads to the change in electrical conductivity of CNC.

Subsequently, B- and N-CNCs have been built in such a way that a C atom of the pentagon tip of CNC is substituted by

Table 2. Adsorption energy of Li on pristine and B/N-doped CNC (E_{ad}), bond reorganization energy (E_{br}, calculated as the energy difference between the geometry of Li after adsorption on nanocone and the full relaxed molecule), NBO charge on the adsorbed Li (Q_T), the HOMO (or SOMO), LUMO and gap in between energies (E_g) for different Li/cone complexes at B3LYP/6-311+G (d). Energies are in eV.

system	E_{ad}	E_{br}	Q_T (e)	*E_{HOMO}	E_{LUMO}	E_g	**ΔE_g(%)
CNC	—	—	—	−5.32	−2.78	2.54	—
Li adsorbed CNC	−0.93	−1.16	0.46	−3.49	−2.73	0.76	70.0
B-CNC	—	—	—	−4.89	−3.88	1.01	—
Li adsorbed B-CNC	−2.19	−2.50	0.33	−4.82	−2.70	2.10	107.9
N-CNC	—	—	—	−3.87	−2.96	0.91	—
Li adsorbed N-CNC	−0.46	−0.58	0.39	−3.64	−2.81	0.83	8.8

*It also stands for the energy of SOMO.
**Change of E_g of cone after the adsorption of Li atom.

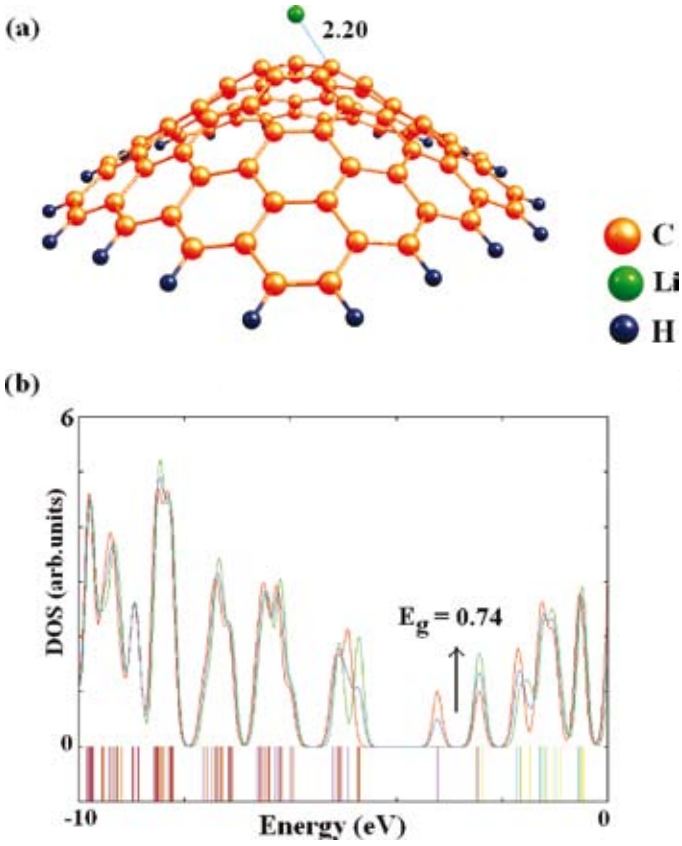

Fig. 2. Optimized structure of Li atom adsorbed on pristine CNC and its DOS plot. Distance is in Å.

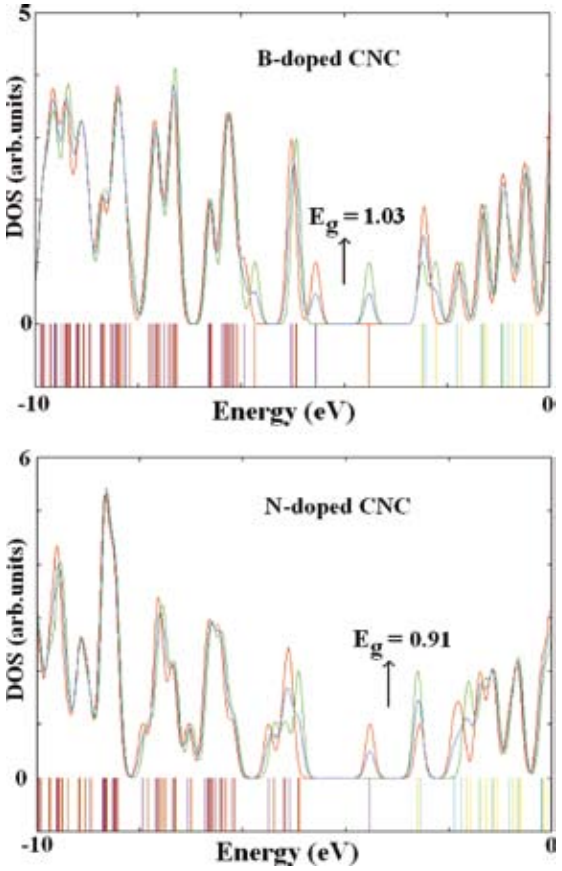

Fig. 3. Comparison between the DOSs of the B- and N-doped CNC.

B and N atoms, respectively. When a B atom is doped in CNC, the E_{dop} is calculated to be +2.50 eV, but it is found to be +0.23 eV for N-doping process. These positive values indicate that both of the doping processes are endothermic and also suggest that the N-doping may be a more energetically favorable process than B-doping. In the doped CNCs, the B-involving bonds become longer (1.49-1.52 Å), and N-involving bonds have no apparent changes; therefore, the B-doped CNC swells slightly outward. Calculated DOS of B- and N-CNCs are shown in Fig. 3, indicating that their E_g values are reduced to 1.03 eV and 0.91 eV respectively, compared to the pristine CNC. However, the B-doping forms an acceptor-like level and N-doping a donor-like one, revealing that doping semiconductive CNCs with B or N atoms will create a *p*- or *n*-type semiconductive material which results in an increased conductivity.

The most stable configurations of a Li atom adsorbed on the top of the pentagonal ring of B- and N-CNCs are shown in Fig. 4. Compared to the pristine CNC, B or N doping dramatically changes the E_{ad} of a Li atom from −1.08 (for CNC) to −2.49 eV (for B-CNC) and −0.55 eV (for N-CNC). B impurity would improve the Li adsorption, but N impurity has negative effects on the Li adsorption. It can be rationalized by the fact that N atom contains an electron pair and B atom has empty p orbital, so they act as Lewis base and acid, respectively. However, it is obvious that Li atom with an electron in its p orbital acts as a Lewis base which interacts more favorably with B site of the B-CNC. In the Li/N-CNC, a local structural deformation at the adsorption site can be observed, where the C5–N–C5 angle is decreased from 107.5° to 105.2° and the N–C5 and N–C6 bond lengths are about 1.43 and 1.44 Å, respectively. Thus, the symmetry properties of N-CNC were significantly affected after the intercalation of Li atom. Unlike N-CNC, structural deformation in Li intercalated B-CNC is negligible and the symmetry of B-CNC remained almost unchanged after Li adsorption.

Also, more favorable adsorption of Li on B-CNC compared to pristine cone can be interpreted by our frontier molecular analysis which reveals that a SOMO/SOMO overlap may be responsible for this favorable interaction. Fig. 5 shows that the SOMO of B-CNC on its B atom. It suggests that the SOMO of Li atom with an unpaired electron strongly interacts with that of B-CNC with one electron again, creating the HOMO and LUMO of Li/B-CNC complex. Based on the NBO charge analysis, the charges of C, B, and N in pristine, B- and N- CNC are −0.077 *e*, −0.004 *e* and −0.719 *e*, respectively. As a result, B-doping forms a localized electron-deficient structure in CNC, but N-doping forms an electron-rich structure.

According to calculated DOSs in Fig. 4, there are electronically obvious changes in the E_g for the B- or N-CNC after Li adsorption (by about 102.8% and 9.9% change in the E_g, respectively). According to this figure, the effect of Li adsorption on the electronic properties of B- and N-CNC is in

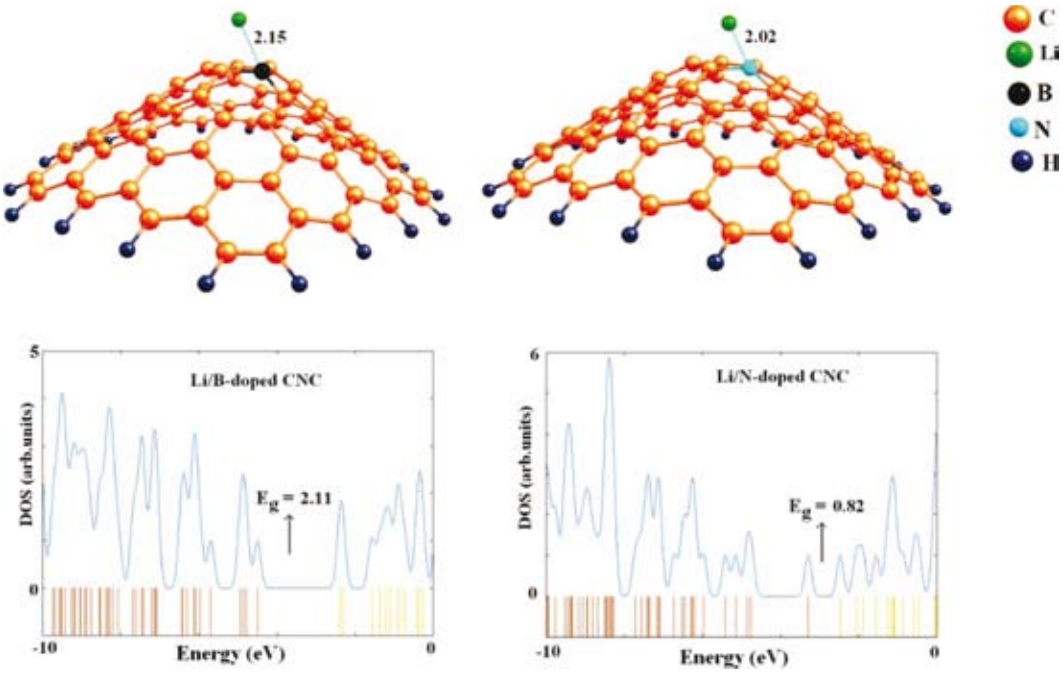

Fig. 4. Optimized structure of Li atom adsorbed on B- and N-doped CNC and their DOS plots. Distances are in Å.

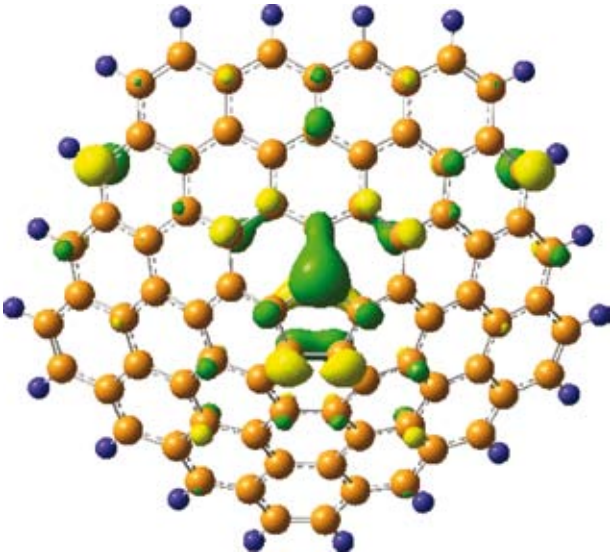

Fig. 5. SOMO (single occupied molecular orbital) profiles of B-doped carbon nanocone.

different pattern. Its adsorption on the B- and N-CNC leads to an increase and decrease in the E_g value by about 1.08 and 0.09 eV, respectively. It seems that Li atom acts as an electron-donor agent with n-type effect on these semiconductors. Therefore, its adsorption on the B-CNC somewhat compensates the p-type effect of B-doping, so that the E_g value of system approximately returns to its initial value in the pristine CNC. On the contrary, the adsorption process on the N-CNC nearly promotes the n-type effect of N-doping, leading to more reduced E_g value. On comparison, Zhou *et al.*, using a DFT-GGA approach, have investigated the lithium adsorption energies and electronic structures of B or N-doped CNTs as well as their potential application in Li batteries [29]. They found that Li adsorption on pristine (5,5) CNT is an endothermic process with positive E_{ad}, whereas the boron doping can stabilize the Li adsorption on the tube walls with negative E_{ad} of −0.73 eV; however, N-doping forms an electron-rich structure, and will hinder the Li adsorption in CNT.

Finally, we have explored the effect of basis set on the obtained results. Therefore, we have repeated all of the energy calculations using 6-311++G(d, p) basis set. The results have been summarized in Table 2, showing that the E_{ad} values of this basis set are slightly less negative than those of the smaller one. As shown in table 2, although the results related to the energies of HOMO, LUMO, Fermi level and E_g are slightly changed by changing the basis set, there are still dramatic changes in the E_g for the pristine and B-CNCs after Li adsorption similar to the results of 6-31G(d) basis set.

Conclusion

We performed DFT calculations on the adsorption of a Li atom on the pristine, B- and N- CNCs. We have shown that the Li atom is strongly adsorbed above the center of the pentagonal ring of the pristine CNC, releasing energy of 1.08 eV (at B3LYP/6-31G (d)), so that the semiconductive CNC is transformed to an n-type one. The B-doping in the tip of CNC improves the Li adsorption, while the N-doping hinders this process. It seems that Li atom acts as an electron-donor agent with n-type effect, therefore, its adsorption on the B-CNC

somewhat compensates the p-type effect of B-doping, so that the E_g value of the system approximately returns to its initial value. The B-doping increases the capacity of CNC toward Li atoms, suggesting that the B-CNCs might be candidates for the anode material in battery applications.

References

1. Migge S.; Sandmann, G; Rahner, D; Dietz, H; Plieth, W. *J. Solid State Electrochem*. **2005**, *9*, 132-137.
2. Li, W.J.; Fu, Z.W. *Appl. Surf. Sci*. **2010**, *256*, 2447-2452.
3. Nithya, V.D.; Selvan, R.K.; Vediappan, K.; Sharmila, S.; Lee, C.W. *Appl. Surf. Sci*. **2012**, *261*, 515-519.
4. Li, G.; Zhang, J. *Appl. Surf. Sci*. **2012**, *258*, 7612-7616.
5. Dresselhaus, M.S.; Dresselhaus, G. *Adv. Phys*. **1981**, *30*, 139-326.
6. Winter, M.; Besenhard, J.O.; Spahr, M.E.; Novak, P. *Adv. Mater*. **1998**, *10*, 725-763.
7. Dahn, J.R.; Zheng, T.; Liu, Y.; Xue, J.S. *Science* **1995**, *270*, 590-593.
8. Maurin, G.; Bousquet, C.; Henn, F.; Bernier, P.; Almairac, R.; Simon, B. *Chem. Phys. Lett*. **1999**, *312*, 14-18.
9. Gao, B.; Kleinhammes, A.; Tang, X.P.; Bower, C.; Fleming, L.; Wu, Y.; Zhou, O. *Chem. Phys. Lett.* **1999**, *307*, 153-157.
10. Gao, B.; Bower, C.; Lorentzen, J.D.; Fleming, L.; Kleinhammes, A.; Tang, X.P.; McNeil, L.E.; Wu, Y.; Zhou, O. *Chem. Phys. Lett*. **2000**, *327*, 69-75.
11. Zhao, J.; Buldum, A.; Han, J.; Lu, J.P. *Phys. Rev. Lett*. **2000**, *85*, 1706-1709.
12. Kurita, N. *Carbon* **2000**, *38*, 65-75.
13. Endo, M.; Hayashi, T.; Hong, S.H.; Enoki, T.; Dresselhaus, M.S. *J. Appl. Phys*. **2001**, *90*, 5670-5674.
14. Stournara, M.E.; Shenoy, V.B. *J. Power Sources* **2011**, *196*, 5697-5703.
15. Fan, S.; Sun, T.; Rui, X.; Yan, Q.; Hang, H.H. *J. Power Sources* **2012**, *201*, 288-293.
16. Iijima, S. *Nature* **1991**, *354*, 56-58.
17. Rogel-Hernandez, E.; Alonso-Nonez, G.; Camarena, J.P.; Espinoza-Gomez, G.A.; Paraguay-Delgado, P.; Somanathan, R. *J. Mex. Chem. Soc*. **2011**, *55*, 7-10.
18. Alonso, J.A.; Cabria, I.; Lopez, M.J. *J. Mex. Chem. Soc*. **2012**, *56*, 261-269.
19. Beheshtian, J.; Ahmadi Peyghan, A.; Bagheri, Z., *J. Mol. model.* **2012**, *19*, 255-261.
20. Beheshtian, J.; Peyghan, A. A.; Bagheri, Z. *Monatshefte für Chemie*/Chemical Monthly **2012**, 143, 1623-1626.
21. Beheshtian, J.; Peyghan, A. A.; Bagheri, Z. *J. Mol. model.* **2012**, *19*, 391-396.
22. Iijima, S.; Ichihashi, T.; Ando, Y. *Nature*, **1992**, *356*,776-778.
23. Pincak, R.; Osipov, V.A. *Phys. Lett. A* **2003**, *314*, 315-321.
24. Charlier, J.C.; Rignanese, G.M. *Phys. Rev. Lett*. **2001**, *86*, 5970-5973.
25. Baei, M. T.; Peyghan, A. A.; Bagheri, Z.; Tabar, M. B. *Phys. Lett. A* **2012**, *377*, 107-111.
26. Yu, X.; Tverdal, M.; Raaen, S.; Helgesen, G.; Knudsen, K.D. *Appl. Surf. Sci*. **2008**, *255*, 1906-1910.
27. Wang, Q.; Gao, R.X.; Qu, S.L.; Li, J.J.; Gu, C.Z. *Nanotechnology* **2009**, *20*, 145201-145207.
28. Baei, M. T.; Peyghan, A. A.; Bagheri, Z., Struct. Chemi. **2013**, doi:10.1007/s11224-012-0139-3.
29. Zhou, Z.; Gao, X.; Yan, J.; Song, D.; Morinaga, M. *Carbon* **2004**, *42*, 2677-2682.
30. Pan, S.; Banerjee, S.; Chattaraj, P.K. *J. Mex. Chem. Soc*. **2012**, *56*, 229-240.
31. Gan L. H.; Zhao J. Q. *Physica E* **2009**, 41, 1249-1252.
32. Owens F. *J. Mater. Lett.* **2007**, 61, 1997-1999.
33. de Menezes V. M.; Fagan S. B.; Zanella I.; Mota R. *Microelectron. J.* **2009,** 40, 877-879.
34. Ramírez-Solís A.; Kirtman B.; Bernal-Jáquez R.; Zicovich-Wilson C. M. *J. Chem. Phys.* **2009**, 130, 164904-164912.
35. Schmidt, M. *J. Comput. Chem*. **1993**, *14*, 1347-1363.
36. Krishnan, A.; Dujardin, E.J.; Treacy, M.M.J.; Hugdahl, J.; Lynum, S.; Ebbesen, T.W. *Nature* **1997**, *388*, 451-454.
37. Qu, C.Q.; Qiao, L.; Wang, C.; Yu, S.S.; Jiang, Q.; Zheng, W.T. *Phys. Lett. A* **2010**, *374*, 782-787.
38. Li, S. Semiconductor Physical Electronics, Second ed., springer, USA, **2006**.